


Soft pattern of Rutherford scattering from heavy target mass expansion*

Yu Jia (贾宇)^{1,2†} Jia-Yue Zhang (张佳玥)^{1,2‡} 

¹Institute of High Energy Physics and Theoretical Physics Center for Science Facilities, Chinese Academy of Sciences, Beijing 100049, China

²School of Physics, University of Chinese Academy of Sciences, Beijing 100049, China

Abstract: We investigate the soft behavior of the tree-level Rutherford scattering process. We consider two types of Rutherford scattering processes: One in which a low-energy massless point-like projectile (say, a spin-1/2 or spin-0 electron) hits a static massive composite target particle carrying various spins (up to spin-2), and one where a slowly-moving light projectile hits a heavy static composite target. For the first type, the unpolarized cross sections in the laboratory frame are found to exhibit universal forms in the first two orders of $1/M$ expansion yet differ at the next-to-next-to-leading order (though some terms at this order still remain universal or depend on the target spin in a definite manner). For the second type, at the lowest order in electron velocity expansion, through all orders in $1/M$, the unpolarized cross section is universal (also not sensitive to the projectile spin). The universality partially breaks down at relative order- v^2/M^2 , though some terms at this order are still universal or depend on the target spin in a specific manner. We also employ the effective field theory approach to reproduce the soft behavior of the differential cross sections for when the target particle is a composite spin-1/2 fermion.

Keywords: Rutherford scattering, nucleus structure, heavy quark effective theory, NRQED

DOI: 10.1088/1674-1137/acdb56 **CSTR:** 32044.14.ChinesePhysicsC.49033102

I. INTRODUCTION

Rutherford scattering is one of the most classic experiments in the history of physics. Originally, Geiger and Marsden bombarded a gold foil with a nonrelativistic α particle beam in 1909[1]. Shortly after, in 1911, Rutherford introduced the revolutionary concept of the atomic nucleus and successfully explained the unexpected large-angle rebounding events by simply exploiting classical mechanics[2]. Without exaggeration, the Rutherford scattering experiment heralded the advent of nuclear physics and quantum mechanics.

In the late 1950s, a new form of the Rutherford scattering experiment conducted by McAllister and Hofstadter, that is, bombarding proton and α targets with a 188 MeV electron beam, played a pivotal role in unraveling the nuclear structure[3, 4]. Through ep elastic scattering experiments, the electromagnetic form factors (FFs) of the proton have been measured over a large range of Q^2 (for comprehensive review see [5, 6]). From their profiles at the lower Q^2 end, one can infer the proton's gross features, such as the charge radius and magnetic dipole

[7-9]. It is interesting to note the decade-long puzzle regarding the proton's charge radius [10-12], that is, the five standard discrepancy between the value extracted from ep elastic scattering/ordinary hydrogen spectra and from muonic hydrogen Lamb shift measurement [13, 14].

To infer the gross features of a composite nucleus from elastic Rutherford scattering, the exchanged photon necessarily carries a long wavelength and hence bears low resolution. To this purpose, it is helpful to concentrate on the low-energy Rutherford scattering process exemplified by the pioneering Hofstadter's experiment[3]. It is worth mentioning that another basic QED process, Compton scattering, in which a photon beam shines on a composite spinning target particle, can also be used to probe the internal structure of the atomic nucleus [15]. The angular distribution of Compton scattering in the laboratory frame in the soft photon limit has been thoroughly studied by Gell-Mann and Low in the 1960[16, 17], which turns out to possess some simple and universal structures. Based on the intuitive multipole expansion picture, one naturally anticipates that the soft limit of Rutherford scattering may also exhibit some universal

Received 2 June 2023; Accepted 5 June 2023; Published online 6 June 2023

* Supported in part by the National Natural Science Foundation of China (11925506, 12475090).

† E-mail: jiay@ihep.ac.cn

‡ E-mail: zhangjiayue@ihep.ac.cn



Content from this work may be used under the terms of the Creative Commons Attribution 3.0 licence. Any further distribution of this work must maintain attribution to the author(s) and the title of the work, journal citation and DOI. Article funded by SCOAP³ and published under licence by Chinese Physical Society and the Institute of High Energy Physics of the Chinese Academy of Sciences and the Institute of Modern Physics of the Chinese Academy of Sciences and IOP Publishing Ltd

and recognizable patterns.

The goal of this study is to comprehensively investigate the soft behavior of two typical categories of Rutherford scattering, that is, processes in which a low-energy massless or a slowly-moving light projectile hits a heavy, static, composite spinning target. For simplicity, we assume the projectile to be a structureless point particle, a spin- $\frac{1}{2}$ or spin-0 electron. For concreteness, we choose the spin of the composite target particle to range from 0 to 2. We find in both cases that the differential cross sections of the Rutherford scattering processes possess the universal form in the first two terms upon heavy target mass expansion yet differ at the next-to-next-to-leading order (NNLO) (depending on the target spin). We conjecture that this pattern may persist for a heavy target particle with arbitrary spin.

The rest of the paper is structured as follows: In Section II, we present the expression of the tree-level Rutherford scattering amplitude involving a heavy composite spinning target particle and specify the parameterization of the electromagnetic FFs of various target particles. Section III is the main body of the paper, where we present the soft behavior of two types of unpolarized Rutherford scattering cross sections up to NNLO in heavy target mass expansion, assuming the projectile to be a point spin-1/2 electron. For the first type of Rutherford scattering, the first two terms in the differential cross section upon heavy target mass expansion are universal, and the NNLO term starts to exhibit spin-dependence, but with an interesting pattern. For the second type of Rutherford scattering, we observe that the differential cross section is universal at the lowest order in the velocity of the incident slowly-moving projectile, but to all orders in $1/M$ expansion. At the next-to-leading order (NLO) in projectile velocity, we demonstrate that the first two terms in heavy target mass expansion remain universal, and the NNLO term ($O(v^2/M^2)$ term) exhibits some interesting patterns of target spin dependence. In Section IV, for both types of Rutherford scattering, we attempt to apply heavy particle effective theory (HPET) as well as nonrelativistic QED (NRQED) to reproduce the observed soft behaviors, assuming the target to be a composite spin-1/2 fermion. We summarize the study in Section V. In the appendix, we demonstrate that the observed soft pattern of Rutherford scattering still holds once the projectile is replaced by a point-like spinless electron.

II. AMPLITUDE OF RUTHERFORD SCATTERING INVOLVING A HEAVY COMPOSITE TARGET PARTICLE

To be specific, let us consider the Rutherford scattering process $e(k)N(p) \rightarrow e(k')N(p')$, where N represents a heavy target particle. At the tree-level, Rutherford scattering is induced by a single photon t -channel exchange, as depicted in Fig. 1. The scattering amplitude can be written as

$$\mathcal{M} = \frac{e^2 g_{\mu\nu}}{q^2} \langle e^-(k') | J^\mu | e^-(k) \rangle \langle N(p', \lambda') | J^\nu | N(p, \lambda) \rangle, \quad (1)$$

where J^μ denotes the electromagnetic current, $q = k - k'$ represents the momentum exchange due to the virtual photon, and λ, λ' denote the polarization indices for the massive spinning target particle. For simplicity, we suppress the spin index of the electron.

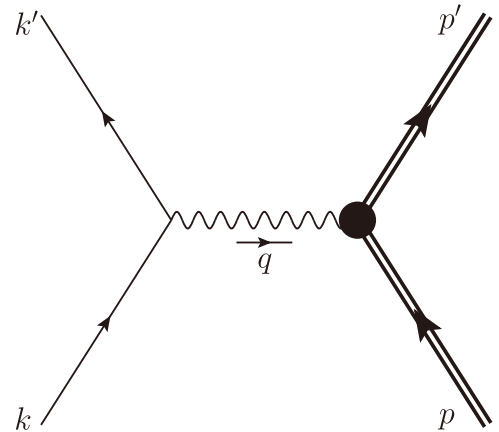


Fig. 1. Tree-level Feynman diagram of the Rutherford scattering process $eN \rightarrow eN$. The double line represents the heavy target particle, and the black dot denotes the electromagnetic vertex given in (2).

The electromagnetic transition matrix element involving the nucleus in (1) is generally a nonperturbative object because the heavy target N is assumed to be any massive composite particle. However, this matrix element can be generally decomposed into a linear combination of independent electromagnetic FFs according to Lorentz group representation [18]:

$$\langle N(p', \lambda') | J^\mu | N(p, \lambda) \rangle_{s=0} = 2P^\mu F_{1,0} \left(\frac{q^2}{M^2} \right), \quad (2a)$$

$$\langle N(p', \lambda') | J^\mu | N(p, \lambda) \rangle_{s=\frac{1}{2}} = \bar{u}(p', \lambda') \left[2P^\mu F_{1,0} \left(\frac{q^2}{M^2} \right) + i\sigma^{\mu\nu} q_\nu F_{2,0} \left(\frac{q^2}{M^2} \right) \right] u(p, \lambda), \quad (2b)$$

$$\begin{aligned} \langle N(p', \lambda') | J^\mu | N(p, \lambda) \rangle_{s=1} = & -\varepsilon_{\alpha'}^*(p', \lambda') \left\{ 2P^\mu \left[g^{\alpha' \alpha} F_{1,0} \left(\frac{q^2}{M^2} \right) - \frac{q^{\alpha'} q^\alpha}{2M^2} F_{1,1} \left(\frac{q^2}{M^2} \right) \right] \right. \\ & \left. - (g^{\mu\alpha'} q^\alpha - g^{\mu\alpha} q^{\alpha'}) F_{2,0} \left(\frac{q^2}{M^2} \right) \right\} \varepsilon_\alpha(p, \lambda), \end{aligned} \quad (2c)$$

$$\begin{aligned} \langle N(p', \lambda') | J^\mu | N(p, \lambda) \rangle_{s=\frac{3}{2}} = & -\bar{u}_{\alpha'}(p', \lambda') \left\{ 2P^\mu \left[g^{\alpha' \alpha} F_{1,0} \left(\frac{q^2}{M^2} \right) - \frac{q^{\alpha'} q^\alpha}{2M^2} F_{1,1} \left(\frac{q^2}{M^2} \right) \right] \right. \\ & \left. + i\sigma^{\mu\nu} q_\nu \left[g^{\alpha' \alpha} F_{2,0} \left(\frac{q^2}{M^2} \right) - \frac{q^{\alpha'} q^\alpha}{2M^2} F_{2,1} \left(\frac{q^2}{M^2} \right) \right] \right\} u_\alpha(p, \lambda), \end{aligned} \quad (2d)$$

$$\begin{aligned} \langle N(p', \lambda') | J^\mu | N(p, \lambda) \rangle_{s=2} = & \varepsilon_{\alpha'_1 \alpha'_2}^*(p', \lambda') \left\{ 2P^\mu \left[g^{\alpha'_1 \alpha_1} g^{\alpha'_2 \alpha_2} F_{1,0} \left(\frac{q^2}{M^2} \right) - \frac{q^{\alpha'_1} q^{\alpha_1}}{2M^2} g^{\alpha'_2 \alpha_2} F_{1,1} \left(\frac{q^2}{M^2} \right) \right] \right. \\ & \left. + \frac{q^{\alpha'_1} q^{\alpha_1}}{2M^2} \frac{q^{\alpha'_2} q^{\alpha_2}}{2M^2} F_{1,2} \left(\frac{q^2}{M^2} \right) \right] - (g^{\mu\alpha'_2} q^{\alpha_2} - g^{\mu\alpha_2} q^{\alpha'_2}) \\ & \times \left[g^{\alpha'_1 \alpha_1} F_{2,0} \left(\frac{q^2}{M^2} \right) - \frac{q^{\alpha'_1} q^{\alpha_1}}{2M^2} F_{2,1} \left(\frac{q^2}{M^2} \right) \right] \left. \right\} \varepsilon_{\alpha_1 \alpha_2}(p, \lambda). \end{aligned} \quad (2e)$$

The various electromagnetic FFs are normalized to be dimensionless. $P = (p + p')/2$ is the average momentum of the target particle, and M is the mass of the target particle. u , ε^μ , u^μ , and $\varepsilon^{\alpha\beta}$ denote the wave function for the spin-1/2, 1, 3/2, and 2 particles, respectively. Only keeping the Lorentz structures that obey the current conservation, we find that the number of independent electromagnetic FFs is $2s + 1$ for the target particle with spin s . Note that the decomposition of the electromagnetic transition matrix element involving a charged particle carrying various spins has been widely studied [19-21].

The electromagnetic FFs in (2) encode the internal structure of the composite target particle. In principle, they can be extracted from experiments or computed using nonperturbative theoretical tools. Although the concrete profiles of various FFs depend on the specific target particle, their values near the zero momentum transfer characterize the electromagnetic multipole moments of the composite target particle. For example, $F_{1,0}(0) = Z$ denotes the total electric charge of the target particle in units of e . $F_{1,0}(0) + F_{1,1}(0)$, $F_{2,0}(0)$, and $F_{2,0}(0) + F_{2,1}(0)$ are the electric quadrupole moment, magnetic dipole moment, and magnetic octupole moment of the composite target particle, in units of $\frac{e}{2M}$, $\frac{e}{M^2}$, and $\frac{e}{2M^3}$, respectively[22]. The charge radius of a proton can also be expressed as $\langle r_p^2 \rangle = \frac{3}{2M^2} [-F_{1,0}(0) + 4F'_{1,0}(0) + F_{2,0}(0)]^D$. It is worth noting that the commonly used electromagnetic FFs of the proton are the Sachs FFs[23, 24], which are defined as

$$G_E \left(\frac{q^2}{M^2} \right) = \left(1 - \frac{q^2}{4M^2} \right) F_{1,0} \left(\frac{q^2}{M^2} \right) + \frac{q^2}{4M^2} F_{2,0} \left(\frac{q^2}{M^2} \right), \quad (3a)$$

$$G_M \left(\frac{q^2}{M^2} \right) = F_{2,0} \left(\frac{q^2}{M^2} \right). \quad (3b)$$

The proton charge radius is defined by $\langle r_p^2 \rangle = \frac{6}{M^2} G'_E(0)$.

III. LOW-ENERGY RUTHERFORD SCATTERING IN HEAVY TARGET MASS EXPANSION

Squaring amplitude (1), averaging over spins in the initial state, and summing over the polarizations in the final states, we can straightforwardly obtain the unpolarized differential cross sections of Rutherford scattering in the laboratory frame for various target particle species. In deriving the unpolarized cross sections, the following spin sum relations are useful:

$$\sum_\lambda u(p, \lambda) \bar{u}(p, \lambda) = \frac{\not{p} + M}{2M}, \quad (4a)$$

$$\sum_\lambda \varepsilon_\alpha(p, \lambda) \varepsilon_{\alpha'}^*(p, \lambda) = \eta_{\alpha\alpha'}, \quad (4b)$$

$$\sum_\lambda u_\alpha(p, \lambda) \bar{u}_{\alpha'}(p, \lambda)$$

1) The Taylor expansion of the form factors around the origin is understood as $F_n(q^2/M^2) = F_n(0) + F'_n(0) \frac{q^2}{M^2} + O(1/M^4)$.

$$= -\frac{\not{p} + M}{2M} \left(g_{\alpha\alpha'} - \frac{1}{3} \gamma_\alpha \gamma_{\alpha'} - \frac{2p_\alpha p_{\alpha'}}{3M^2} + \frac{\gamma_{\alpha'} p_\alpha - \gamma_\alpha p_{\alpha'}}{3M} \right), \quad (4c)$$

$$\sum_\lambda \varepsilon_{\alpha_1 \alpha_2}(p, \lambda) \varepsilon_{\alpha'_1 \alpha'_2}^*(p, \lambda) = \eta_{\alpha_1 \alpha'_1} \eta_{\alpha_2 \alpha'_2} + \eta_{\alpha_1 \alpha'_2} \eta_{\alpha_2 \alpha'_1} - \frac{2}{3} \eta_{\alpha_1 \alpha_2} \eta_{\alpha'_1 \alpha'_2}, \quad (4d)$$

with $\eta_{\alpha\beta} \equiv -g_{\alpha\beta} + \frac{p_\alpha p_\beta}{M^2}$. Note the Dirac spinor wave function is normalized as $\bar{u}(p, r)u(p, s) = \delta^{rs}$.

A. Massless spin-1/2 projectile

We first consider the ep elastic scattering experiment, with the famous Hofstadter's experiment as the prototype [3]. In such cases, the incident electron is treated as massless, and we are concerned with the low-energy limit $|\mathbf{k}| \ll M$.

We focus on Rutherford scattering in the laboratory frame, with the four-momentum of the target particle in the initial state signified by $p^\mu = (M, \mathbf{0})$. The corresponding differential unpolarized cross section is defined by

$$\frac{d\sigma}{d\cos\theta} = \frac{1}{2|\mathbf{k}|} \cdot \frac{1}{2M} \cdot \frac{\mathbf{k}'^2}{8\pi|\mathbf{k}|M} \left(\frac{1}{2} \frac{1}{2s+1} \sum_{\text{spins}} |\mathcal{M}|^2 \right), \quad (5)$$

where θ denotes the polar angle between the incident and reflected electron, and $|\mathbf{k}'|$ is a function of $|\mathbf{k}|$, $\cos\theta$, and M :

$$|\mathbf{k}'| = \frac{|\mathbf{k}|}{1 + \frac{|\mathbf{k}|}{M}(1 - \cos\theta)}. \quad (6)$$

The full expressions of the unpolarized cross sections are generally lengthy and appear cumbersome, and therefore it is difficult to recognize any clear pattern regarding the dependence on the heavy target particle spin. Hopefully, once heavy target mass expansion is conducted, the soft behavior of Rutherford scattering will become transparent and we may readily identify a simple pattern.

After expanding both the squared amplitude and phase space measure (the factor $\mathbf{k}'^2/\mathbf{k}^2$) in the (5) powers of $1/M$, the differential Rutherford scattering cross sections become considerably simpler. We find that the first two orders in heavy target expansion are universal, for example, independent of the heavy target spin,

$$\frac{d\sigma}{d\cos\theta} = \frac{\pi\alpha^2 Z^2 \cos^2 \frac{\theta}{2}}{2\mathbf{k}^2 \sin^4 \left(\frac{\theta}{2} \right)} - \frac{\pi\alpha^2 Z^2 \cos^2 \frac{\theta}{2}}{M|\mathbf{k}| \sin^2 \left(\frac{\theta}{2} \right)} + \mathcal{O} \left(\frac{1}{M^2} \right). \quad (7)$$

For clarity, we substitute $F_{1,0} = Z$. The result is intuitively clear: In the soft limit, the long wavelength photon can only feel the total charge of the composite target particle and is insensitive to any further details about its internal structure.

In contrast, the NNLO terms in heavy target mass expansion vary with different heavy target particles:

$$\left(\frac{d\sigma}{d\cos\theta} \right)_{\text{NNLO}}^s = -\frac{4\pi\alpha^2}{M^2 \sin^2 \frac{\theta}{2}} \left\{ \Theta \left(s - \frac{1}{2} \right) \frac{s+1}{48s} F_{2,0}^2 (\cos\theta - 3) + \frac{1}{4} \cos^2 \frac{\theta}{2} \left[4F'_{1,0} Z - \Theta(s-1) \frac{2}{3} F_{1,1} Z \right. \right. \\ \left. \left. + \Theta \left(s - \frac{1}{2} \right) \frac{5 - (-1)^{2s}}{6} F_{2,0} Z + Z^2 \cos\theta - \frac{1}{3} ([s] + s + 3) Z^2 \right] \right\}, \quad \left(s = 0, \frac{1}{2}, 1, \frac{3}{2}, 2 \right) \quad (8)$$

where $\Theta(s)$ is the Heaviside step function with $\Theta(0) = 1$, and $[s]$ denotes the ceiling function mapping s to the least integer greater than or equal to s . For notational brevity, we neglect the argument 0 in various FFs. We observe that the $F'_{1,0} Z$, $Z^2 \cos\theta$, and $F_{1,1} Z$ terms with a prefactor $\cos^2(\theta/2)$ are still universal, that is, independent of the target spin. In fact, the $F'_{1,0} Z$ and $Z^2 \cos\theta$ terms have the same origin of the leading order (LO) and NLO cross sections, which correspond to different terms in the Taylor expansion of $F_{1,0}^2(q^2/M^2)$ in the squared LO amplitude and phase space measure. The coefficient of the $F_{2,0} Z$ term seems to reflect the spin-statistic characteristic of the target particle. For fermions, the coefficient is 1, whereas for bosons, it is $2/3$.

Although the coefficients of $F_{2,0}^2(\cos\theta - 3)$ inside the

bracket depend on the target particle spin s , they seem to fit into the expression $\frac{1+s}{48s}$ (for $s = 1/2, 1, 3/2, 2$). It will be interesting to see whether this pattern still persists for higher target spin.

Owing to tremendous phenomenological interest, it is interesting to specialize in the spin-1/2 target. Upon heavy target mass expansion, the differential ep elastic scattering cross section can be expressed in terms of the Sachs FFs:

$$\frac{d\sigma}{d\cos\theta} = \frac{\pi\alpha^2 \cos^2 \frac{\theta}{2}}{2\mathbf{k}^2 \sin^4 \left(\frac{\theta}{2} \right)} - \frac{\pi\alpha^2 \cos^2 \frac{\theta}{2}}{M|\mathbf{k}| \sin^2 \left(\frac{\theta}{2} \right)} - \frac{4\pi\alpha^2}{M^2 \sin^2 \frac{\theta}{2}}$$

$$\times \left[\frac{1}{16} G_M^2 (\cos \theta - 3) + \frac{1}{4} \cos^2 \frac{\theta}{2} \left(4G'_E + \cos \theta - \frac{1}{2} \right) \right], \quad (9)$$

or equivalently, expressed in terms of proton charge radius and magnetic dipole moment μ_p by making the replacements $G_M \rightarrow \mu_p$ and $G'_E \rightarrow \frac{\mu_p^2}{6} \langle r_p^2 \rangle$. The contributions of $\langle r_p^2 \rangle$ and μ_p begin at NNLO in heavy target mass expansion, whose values may be extracted by carefully studying the angular distributions.

B. Light non-relativistic spin-1/2 projectile

Next, we turn to the soft limit of the original prototype of the Rutherford scattering process, that is, a slowly moving light particle hits a heavy static target. We again assume that the projectile is a Dirac fermion, whose mass and momentum are denoted by m and \mathbf{k} .

The differential cross section for this type of Rutherford scattering in the laboratory frame is defined by

ford scattering in the laboratory frame is defined by

$$\frac{d\sigma}{d\cos\theta} = \frac{1}{32\pi M} \left[p'^0 + k'^0 \left(1 - \frac{|\mathbf{k}|}{|\mathbf{k}'|} \cos\theta \right) \right]^{-1} \frac{|\mathbf{k}'|}{|\mathbf{k}|} |\mathcal{M}|^2. \quad (10)$$

The resulting expressions are rather lengthy. Fortunately, we are only interested in its soft behavior. Since there are three widely separated scales in this process, which obey $|\mathbf{k}| \ll m \ll M$, the appropriate way of extracting the soft behavior is to expand the differential cross sections in powers of $v = |\mathbf{k}|/m$ (velocity of the projectile) and $1/M$ simultaneously. The necessity of performing double expansion renders this case somewhat more complicated than the preceding case discussed in Section IIIA.

Interestingly, at the lowest order in velocity yet to all orders in $1/M$, the differential cross sections scale as $1/\mathbf{k}^4$, which takes a uniform form:

$$\begin{aligned} \left(\frac{d\sigma}{d\cos\theta} \right)_{(v^2)}^s &= \frac{2\pi Z^2 \alpha^2}{\mathbf{k}^4} \frac{m^2 (M+m)^2 \left(\sqrt{M^2 - m^2 \sin^2 \theta} + m \cos \theta \right)^2}{M \sqrt{M^2 - m^2 \sin^2 \theta} \left(M - \cos \theta \sqrt{M^2 - m^2 \sin^2 \theta} + m \sin^2 \theta \right)^2} \\ &= \frac{8\pi Z^2 \alpha^2 m^2}{\mathbf{k}^4 \sin^4 \frac{\theta}{2}} - \frac{\pi Z^2 \alpha^2 m^4}{M^2 \mathbf{k}^4} + \mathcal{O} \left(\frac{m^6}{M^4 \mathbf{k}^4} \right). \end{aligned} \quad (11)$$

The LO term is the extremely well-known expression obtained by Rutherford using classical mechanics, dubbed the Rutherford formula.

At NLO in velocity expansion, the differential cross sections scale as $1/\mathbf{k}^2$, whose explicit expressions are still rather complicated and vary with different target species. Nevertheless, once heavy target mass expansion is conducted, a clear pattern emerges:

$$\begin{aligned} \left(\frac{d\sigma}{d\cos\theta} \right)_{(v^2)}^s &= \frac{\pi \alpha^2}{\mathbf{k}^2 \sin^2 \frac{\theta}{2}} \left[\frac{Z^2 \cos^2 \frac{\theta}{2}}{2 \sin^2 \frac{\theta}{2}} - \frac{Z^2 m \cos^2 \frac{\theta}{2}}{M} \right. \\ &\quad \left. - \frac{Zm^2}{4M^2} f_{\text{NNLO}}^s + \mathcal{O} \left(\frac{1}{M^3} \right) \right], \end{aligned} \quad (12)$$

where

$$\begin{aligned} f_{\text{NNLO}}^s &= 16F'_{1,0} + Z \cos \theta - \Theta(s-1) \frac{8}{3} F_{1,1} \\ &\quad + \Theta \left(s - \frac{1}{2} \right) \frac{2[5 - (-1)^{2s}]}{3} F_{2,0} \\ &\quad - \frac{4}{3} \left([s] + s + \frac{3}{4} \right) Z. \quad \left(s = 0, \frac{1}{2}, 1, \frac{3}{2}, 2 \right) \end{aligned} \quad (13)$$

The LO and NLO terms in $1/M$ expansion are universal. The NNLO terms begin to exhibit target spin depend-

ence. However, even at $\mathcal{O}(v^2/M^2)$, the $F'_{1,0}$, $F_{1,1}$, and $Z \cos \theta$ terms still seem to be universal, that is, independent of the target particle spin. The coefficient of $F_{2,0}$ seems to reflect the spin-statistic characteristic of the target particle. For fermions, the coefficient is 4, whereas for bosons, it is $8/3$.

IV. REPRODUCING THE SOFT BEHAVIOR FROM EFFECTIVE FIELD THEORY

The low-energy limit of Rutherford scattering is largely dictated by a heavy target particle interacting with a soft photon. Therefore, it is natural to expect that the soft behavior can be reproduced by an effective field theory (EFT) analogous to heavy quark effective theory (HQET), which automatically incorporates heavy target mass expansion. In this section, we specialize in the case of a spin-1/2 composite target particle.

Originally, HQET was designed to describe a structureless heavy quark interacting with soft gluons [25, 26]. Owing to the asymptotic freedom property of QCD, Wilson coefficients can be computed in perturbation theory through a perturbative matching procedure.

The key idea of HQET can be readily transplanted to the case of a heavy composite particle interacting with a soft photon, as long as the photon wavelength is too long to deeply probe the internal structure of the composite

target. Consequently, one is generally unable to calculate various Wilson coefficients from the top-down perspective. The internal structure of the composite heavy target particle is encoded in various Wilson coefficients, which essentially represent various multipole moments. They can, in principle, be evaluated by nonperturbative means

$$\mathcal{L}_{\text{HPET}} = \bar{h}_v \left(iD_0 + c_2 \frac{\mathbf{D}^2}{2M} + c_F e \frac{\boldsymbol{\sigma} \cdot \mathbf{B}}{2M} + c_D e \frac{[\nabla \cdot \mathbf{E}]}{8M^2} + i c_S e \frac{\boldsymbol{\sigma} \cdot (\mathbf{D} \times \mathbf{E} - \mathbf{E} \times \mathbf{D})}{8M^2} \right) h_v + \mathcal{O}(1/M^3), \quad (14)$$

where we truncate the effective Lagrangian through order $1/M^2$. h_v represents the heavy target HPET field, with the label velocity $v^\mu = (1, \mathbf{0})$, $D^\mu = \partial^\mu + iZeA^\mu$ signifies the covariant derivative, \mathbf{E} and \mathbf{B} denote the electric and magnetic field, the coefficient $c_2 = 1$ is a rigorous consequence of Lorentz symmetry, and the c_F , c_D , and c_S -related terms are often referred to as Fermi, Darwin, and spin-orbital terms. The organization of the HPET Lagrangian is governed by powers of $|\mathbf{q}|/M$, with \mathbf{q} signify-

ing the photon momentum.

or determined using the bottom-up approach, for example, extracted from low-energy Rutherford scattering experiments.

Analogous to HQET, we build up an EFT, dubbed HPET, describing a static heavy composite fermionic target particle interacting with a soft photon:

ing the photon momentum.

A. HPET description of a massless spin-1/2 projectile hitting a static spin-1/2 target

In contrast with Fig. 1, up to order $1/M^2$, there are five Feynman diagrams in the context of HPET for the tree-level process $e(k)N(p) \rightarrow e(k')N(p')$. The corresponding amplitude reads

$$\begin{aligned} \mathcal{M}_{\text{HPET}} = & -\sqrt{1 + c_2 \frac{\mathbf{p}^2}{2M^2}} \frac{e^2}{q^2} \left\{ -Z \bar{u}_{\text{NR}} u_{\text{NR}} \bar{u}(k') \gamma^0 u(k) + \frac{c_2 Z}{2M} \bar{u}_{\text{NR}} u_{\text{NR}} \bar{u}(k') \mathbf{p}' \cdot \boldsymbol{\gamma} u(k) \right. \\ & \left. - \frac{c_F}{4M} \bar{u}_{\text{NR}} [\boldsymbol{q}, \boldsymbol{\gamma}^\mu] u_{\text{NR}} \bar{u}(k') \gamma_\mu u(k) - \frac{c_D q^2}{8M^2} \bar{u}_{\text{NR}} u_{\text{NR}} \bar{u}(k') \gamma^0 u(k) \right\} \\ = & \frac{e^2}{q^2} \left\{ Z \bar{u}_{\text{NR}} u_{\text{NR}} \bar{u}(k') \gamma^0 u(k) + \frac{c_F}{4M} \bar{u}_{\text{NR}} [\boldsymbol{q}, \boldsymbol{\gamma}^\mu] u_{\text{NR}} \bar{u}(k') \gamma_\mu u(k) + \frac{c_D q^2}{8M^2} \bar{u}_{\text{NR}} u_{\text{NR}} \bar{u}(k') \gamma^0 u(k) \right\}, \quad (15) \end{aligned}$$

where u_{NR} denotes the HPET spinor wave function that satisfies $\psi u_{\text{NR}}(v, s) = u_{\text{NR}}(v, s)$ and $\bar{u}_{\text{NR}}(v, s) u_{\text{NR}}(v, s) = 2v^0$. Notice that the final expression does not depend on c_2 . Moreover, note that the contribution from the c_S term is proportional to $q^0 \sim \mathbf{k}^2/M$; hence, it does not need to be considered at the prescribed accuracy of $1/M^2$.

Squaring the amplitude in (15) and summing/averaging over polarizations, we find the differential unpolarized cross section obtained from the HPET side:

$$\begin{aligned} \frac{d\sigma}{d\cos\theta} \Big|_{\text{EFT}} = & \frac{\pi\alpha^2 Z^2 \cos^2 \frac{\theta}{2}}{2\mathbf{k}^2 \sin^4 \frac{\theta}{2}} - \frac{\pi\alpha^2 Z^2 \cos^2 \frac{\theta}{2}}{M|\mathbf{k}| \sin^2 \frac{\theta}{2}} \\ & - \frac{\pi\alpha^2}{8M^2 \sin^2 \frac{\theta}{2}} \left[Z^2 (\cos 2\theta - 1) \right. \\ & \left. + c_D Z (\cos\theta + 1) + c_F^2 (\cos\theta - 3) \right]. \quad (16) \end{aligned}$$

Note that the LO and NLO terms are only sensitive to the total charge Ze of the target particle and do not depend on any nontrivial Wilson coefficients (hence they are insensitive to the target's internal structure). This indicates that these two terms are solely dictated by the

leading HPET Lagrangian. Since the leading HPET Lagrangian possesses heavy particle spin symmetry, the spin degree of freedom is completely decoupled at the lowest order in $1/M$ expansion. From a technical perspective, the first two terms arise solely from expanding the squared LO amplitude in (15) as well as expanding the factor $|\mathbf{k}'|/|\mathbf{k}|$ in the phase space measure in Eq. (10).

At first sight, one may worry that the interference between the c_F term and the LO amplitude would nominally generate a $\mathcal{O}(1/M)$ correction, thus breaking the universality at NLO. A closer examination reveals that this contribution actually vanishes after summing over polarizations. This cancellation is anticipated to persist for other species of spinning target particles.

The first two terms in (16) are indeed identical to the universal behaviors revealed in (7). The EFT approach helps us to better understand why they are independent of the species of the composite target particle, though our HPET Lagrangian only specializes in the spin-1/2 target.

At NNLO in $1/M$ expansion, three terms emerge, which stem from different sources. The first term clearly stems from expanding the squared LO amplitude in combination with phase space expansion, which is of the same origin as the LO and NLO contributions and is anticipated to be universal. The second term comes from the

interference between the c_D term and the LO amplitude, and the last term stems from the square of the c_F term. Concretely, the last two terms depend on the composite target particle's charge radius and magnetic dipole. Interestingly, the c_F term can be identified with the $F_{2,0}^2(\cos\theta - 3)$ term in (8). As discussed in the paragraph

after (8), the coefficient of this term may depend on the target spin in a specific manner.

To verify that the EFT amplitude does capture the correct soft behavior, we can perform heavy target mass expansion from the full QED amplitude in Eq. (1):

$$\begin{aligned} \mathcal{M}_{\text{QED}} &= \frac{e^2}{q^2} \bar{u}(k') \gamma^\mu u(k) \bar{u}(p', \lambda') \left[2P^\mu F_{1,0} \left(\frac{q^2}{M^2} \right) + i\sigma^{\mu\nu} q_\nu F_{2,0} \left(\frac{q^2}{M^2} \right) \right] u(p, \lambda) \\ &= \frac{e^2}{q^2} \bar{u} \gamma^\mu u \bar{u}_{\text{NR}}^{\lambda'} \sqrt{\frac{p'^0}{M}} \left(1 - \frac{\mathbf{p}' \cdot \boldsymbol{\gamma}}{2M} - \frac{\mathbf{p}'^2}{8M^2} \right) \left[2P^\mu \left(F_{1,0} + F'_{1,0} \frac{q^2}{M^2} \right) + i\sigma^{\mu\nu} q_\nu F_{2,0} \right] u_{\text{NR}}^\lambda \\ &= \frac{2Me^2}{q^2} \left[Z \bar{u} \gamma^0 u \bar{u}_{\text{NR}}^{\lambda'} u_{\text{NR}}^\lambda + \frac{F_{2,0}}{4M} \bar{u} \gamma_\mu u \bar{u}_{\text{NR}}^{\lambda'} [\not{q}, \gamma^\mu] u_{\text{NR}}^\lambda + \frac{q^2 (8F'_{1,0} - F_{1,0} + 2F_{2,0})}{8M^2} \bar{u} \gamma^0 u \bar{u}_{\text{NR}}^{\lambda'} u_{\text{NR}}^\lambda \right], \end{aligned} \quad (17)$$

where we not only expand the FF $F_{1,0}$ to the first order in q^2/M^2 , but also expand the Dirac spinor using $u(p') = \sqrt{\frac{p'^0}{M}} \left(1 - \frac{\mathbf{p}' \cdot \boldsymbol{\gamma}}{2M} - \frac{\mathbf{p}'^2}{8M^2} \right) u_{\text{NR}} + \mathcal{O}(1/M^3)$.

Note that the HPET amplitude assumes nonrelativistic normalization for the target particle; therefore, we must include an overall factor $2M$ prior to comparing it with the full QED amplitude. By equating (15) and (17), we are able to identify the relations between the Wilson coefficients in HPET and the electromagnetic FFs near the zero-momentum transfer:

$$c_F = F_{2,0}, \quad (18a)$$

$$c_D = 2F_{2,0} + 8F'_{1,0} - F_{1,0}, \quad (18b)$$

which are identical to the relations obtained for the structureless quark in HQET [27].

Substituting relation (18) into (16), we fully reproduce the NNLO contribution for a heavy spin-1/2 target, as recorded in (8).

B. NRQED+HPET description of a slowly-moving spin-1/2 projectile hitting a static spin-1/2 target

Next, we turn to the EFT approach to understand the

second type of Rutherford scattering, where a light nonrelativistic particle hits a static heavy composite target. To be specific, we specialize in a spin-1/2 structureless projectile and a spin-1/2 target particle. The treatment of the static composite fermionic target is identical to that in Section IV.A. It is natural to apply NRQED [28] to describe the incident slowly-moving electron.

Up to the relative order v^2 , the electron sector of the NRQED Lagrangian reads as

$$\begin{aligned} \mathcal{L}_{\text{NRQED}} &= \psi^\dagger \left[iD^0 + d_2 \frac{\mathbf{D}^2}{2m} + d_4 \frac{\mathbf{D}^4}{8m^3} + d_F e \frac{\boldsymbol{\sigma} \cdot \mathbf{B}}{2m} \right. \\ &\quad \left. + d_D e \frac{[\nabla \cdot \mathbf{E}]}{8m^2} + id_S e \frac{\boldsymbol{\sigma} \cdot (\mathbf{D} \times \mathbf{E} - \mathbf{E} \times \mathbf{D})}{8m^2} \right] \psi, \end{aligned} \quad (19)$$

where ψ denotes a Pauli spinor field that annihilates a nonrelativistic electron, $d_2 = d_4 = 1$ is a rigorous consequence of Lorentz invariance, and the d_4 term, together with the d_F , d_D , and d_S terms (referred to as the Fermi, Darwin, and spin-orbital terms), represent the $\mathcal{O}(v^2)$ corrections to the NRQED Lagrangian. At the tree level, the Wilson coefficients $d_F = d_D = d_S = 1$.

Our starting point is the HPET Lagrangian (14) and the NRQED Lagrangian (19). It is convenient to work in Coulomb gauge. Up to $\mathcal{O}(v^2/M^2)$, the relevant tree-level EFT amplitude for $eN \rightarrow eN$ reads as

$$\begin{aligned} \mathcal{M}_{\text{EFT}} &= \frac{e^2}{q^2} \xi^\dagger \left[1 + \frac{d_2}{4m^2} (\mathbf{k}^2 + \mathbf{k}'^2) - \frac{d_D}{8m^2} |\mathbf{k}' - \mathbf{k}|^2 - \frac{id_S}{4m^2} \boldsymbol{\sigma} \cdot (\mathbf{k} \times \mathbf{k}') \right] \xi \bar{u}_{\text{NR}}^{\lambda'} \left[-Z + \frac{(c_D - 2c_2 Z) \mathbf{p}^2}{8M^2} \right] u_{\text{NR}}^\lambda \\ &\quad - \frac{1}{q^2} \left(\delta^{ij} - \frac{q^i q^j}{\mathbf{q}^2} \right) \xi^\dagger \left\{ (k^i + k'^i) \left[\frac{d_2}{2m} + \frac{d_2^2 - d_4}{8m^3} (\mathbf{k}^2 + \mathbf{k}'^2) \right] + \frac{id_F}{2m} \left(1 + d_2 \frac{\mathbf{k}^2 + \mathbf{k}'^2}{4m^2} \right) [\boldsymbol{\sigma} \times (\mathbf{k}' - \mathbf{k})]^i \right. \\ &\quad \left. - \frac{d_D}{16m^3} (k'^i - k^i) (\mathbf{k}'^2 - \mathbf{k}^2) - \frac{id_S}{16m^3} (\mathbf{k}'^2 - \mathbf{k}^2) [\boldsymbol{\sigma} \times (\mathbf{k} + \mathbf{k}')]^i \right\} \xi \bar{u}_{\text{NR}}^{\lambda'} \left[-\frac{c_2 Z}{2M} p'^j - i \frac{c_F}{2M} \sigma^{jl} p'^l \right] u_{\text{NR}}^\lambda, \end{aligned} \quad (20)$$

where the first line represents temporal photon exchange, and the remaining lines represent transverse photon exchange. ξ denotes the two-component spinor wave function.

After some simplification, (20) reduces to

$$\begin{aligned} \mathcal{M}_{\text{EFT}} = & \frac{e^2}{\mathbf{q}^2} \left[-Z + \frac{(c_D - 2c_2 Z) \mathbf{p}^2}{8M^2} \right] \xi^\dagger \left[1 + \frac{d_2}{4m^2} (\mathbf{k}^2 + \mathbf{k}'^2) - \frac{d_D}{8m^2} |\mathbf{k}' - \mathbf{k}|^2 - \frac{id_S}{4m^2} \boldsymbol{\sigma} \cdot (\mathbf{k} \times \mathbf{k}') \right] \xi \bar{u}_{\text{NR}}^{\lambda'} u_{\text{NR}}^\lambda - \frac{c_F e^2}{4M \mathbf{q}^2} \xi^\dagger \\ & \times \left\{ (k^i + k'^i) \left[\frac{d_2}{2m} + \frac{d_2^2 - d_4}{8m^3} (\mathbf{k}^2 + \mathbf{k}'^2) \right] + \frac{id_F}{2m} [\boldsymbol{\sigma} \times (\mathbf{k}' - \mathbf{k})]^i - \frac{id_S}{16m^3} (\mathbf{k}'^2 - \mathbf{k}^2) [\boldsymbol{\sigma} \times (\mathbf{k}' - \mathbf{k})]^i \right\} \xi \times \bar{u}_{\text{NR}}^{\lambda'} [\gamma^i, \boldsymbol{\gamma} \cdot \mathbf{q}] u_{\text{NR}}^\lambda. \quad (21) \end{aligned}$$

Squaring the amplitude in (21), and summing/averaging over various spins, we obtain the differential unpolarized Rutherford scattering cross section in the context of EFT:

$$\begin{aligned} \left. \frac{d\sigma}{d\cos\theta} \right|_{\text{EFT}} = & \frac{\pi\alpha^2 m^2 Z^2}{2\mathbf{k}^4 \sin^4 \frac{\theta}{2}} - \frac{\pi\alpha^2 m^4 Z^2}{M^2 \mathbf{k}^4} + \frac{\pi\alpha^2 Z}{2\mathbf{k}^2 \sin^2 \frac{\theta}{2}} \left\{ \frac{Z(d_D \cos\theta - d_D + 2)}{2\sin^2 \frac{\theta}{2}} \right. \\ & \left. - \frac{m}{M} (d_D \cos\theta - d_D + 2) - \frac{m^2}{2M^2} [Z(2 + d_D - 4c_2) + Z \cos\theta(2 - d_D) + 2c_D] \right\}. \quad (22) \end{aligned}$$

The d_S term in (21) does not contribute to the squared amplitude because its interference with the LO amplitude in velocity expansion only contains a single Pauli matrix and hence vanishes upon summing over polarization.

Substituting $c_2 = d_D = 1$ in (22), and utilizing the relations given in (18), we exactly reproduce (11), which encodes the LO and NLO terms in heavy target expansion, and (13), which encapsulates the NNLO term. (13) indicates that the $Z \cos\theta$ and $F'_{1,0}$ terms in NNLO correction are universal, for example, independent of the target spin. This may indicate that structures such as $Z \cos\theta(2 - d_D) + 2c_D$ arise ubiquitously in an EFT calculation for heavy targets other than spin-1/2 fermions.

To verify that the EFT amplitude indeed reproduces the correct soft behavior, we conduct both nonrelativistic and heavy target mass expansion from the full QED amplitude in (1).

Working again in the Coulomb gauge, and employing the following relation between the relativistic electron spinor and nonrelativistic electron spinor:

$$u(k) = \frac{1}{\sqrt{k^0 + m}} \begin{pmatrix} (k^0 + m) \xi \\ \mathbf{k} \cdot \boldsymbol{\sigma} \xi \end{pmatrix}, \quad \bar{u}(k) = \frac{1}{\sqrt{k^0 + m}} \left((k^0 + m) \xi^\dagger - \xi^\dagger \mathbf{k} \cdot \boldsymbol{\sigma} \right),$$

we expand the full QED amplitude through $\mathcal{O}(v^2/M^2)$:

$$\begin{aligned} \mathcal{M}_{\text{QED}} = & -\frac{e^2}{\mathbf{q}^2} \bar{u}(k') \gamma^0 u(k) \bar{u}_{\text{NR}}^{\lambda'} \left[2ZP^0 + \frac{P^0}{4M^2} (8F'_{1,0} q^2 + Z\mathbf{q}^2) + i \frac{\mathbf{P}' \cdot \boldsymbol{\gamma}}{2M} \sigma^{0i} q_i F_{2,0} \right] u_{\text{NR}}^\lambda \\ & - \frac{e^2}{\mathbf{q}^2} \left(\delta_{ij} - \frac{q^i q^j}{\mathbf{q}^2} \right) \bar{u} \gamma^i u \bar{u}_{\text{NR}}^{\lambda'} \left[2ZP^j + \frac{1}{2} [q, \gamma^j] F_{2,0} + \frac{P^j}{4M^2} (8F'_{1,0} q^2 + Z\mathbf{q}^2) \right] u_{\text{NR}}^\lambda \\ = & \frac{2Me^2}{\mathbf{q}^2} 2m \left[-Z + \frac{\mathbf{p}'^2}{8M^2} (2F_{2,0} + 8F'_{1,0} - 3Z) \right] \xi^\dagger \left[1 + \frac{|\mathbf{k} + \mathbf{k}'|^2}{8m^2} - \frac{i}{4m^2} \boldsymbol{\sigma} \cdot (\mathbf{k} \times \mathbf{k}') \right] \xi \bar{u}_{\text{NR}}^{\lambda'} u_{\text{NR}}^\lambda \\ & - \frac{F_{2,0} e^2}{2\mathbf{q}^2} 2m \xi^\dagger \left\{ \frac{1}{2m} (k^i + k'^i) + \frac{i}{2m} [\boldsymbol{\sigma} \times (\mathbf{k}' - \mathbf{k})]^i - \frac{i}{16m^3} (\mathbf{k}'^2 - \mathbf{k}^2) [\boldsymbol{\sigma} \times (\mathbf{k}' - \mathbf{k})]^i \right\} \xi \bar{u}_{\text{NR}}^{\lambda'} [\gamma^i, \boldsymbol{\gamma} \cdot \mathbf{q}] u_{\text{NR}}^\lambda. \quad (23) \end{aligned}$$

After including the normalization factor $(2M)(2m)$, employing the relations for the heavy target Wilson coefficients in (18), and taking $d_2 = d_4 = d_F = d_D = d_S = 1$, we find that the EFT amplitude (21) exactly agrees with the full QED amplitude (24).

V. SUMMARY

In this study, we conduct a comprehensive investigation of the soft behavior of the tree-level Rutherford scattering process. We consider two classes of Rutherford

scattering experiments: One in which a low-energy point-like massless projectile (for example, a spin-1/2 or spin-0 electron) bombards a static massive composite spinning target particle (for example, an atomic nucleus), and one where a slowly-moving light structureless projectile hits a static heavy composite spinning target. We consider various composite target particles with spin up to 2.

The soft limit of the differential Rutherford cross sections in the laboratory frame in both cases exhibits some universal pattern. For the first type of Rutherford scattering process, given a specific projectile, the first two terms in the differential cross section are universal upon heavy target mass expansion, whereas the universality starts to break down at NNLO. Nevertheless, many terms at NNLO still remain spin-independent or have some definite spin-dependence pattern. For the second type, we must perform both nonrelativistic and heavy target mass expansion to infer the correct soft limit. At the lowest order in projectile velocity expansion, but to all orders in $1/M$ expansion, the differential cross section has a universal form (insensitive to the projectile spin). At NLO in velocity expansion, the first two terms in the differential cross section in $1/M$ expansion are still universal. The $O(v^2/M^2)$ piece starts to partially violate the universality. Despite this, some terms at this order still remain target spin independent.

It is of special interest that the $F_{2,0}$ term (magnetic dipole of the target particle) at $O(1/M^2)$ (or $O(v^2/M^2)$ for the second type of Rutherford scattering) seems to reflect a peculiar spin-statistics feature. Its coefficient keeps one constant for the fermionic target and another constant for the bosonic target. It is interesting to verify this observation by investigating target particles with even higher spin.

We also attempt to apply the EFT approach to understand the soft pattern of the Rutherford scattering cross

sections, taking the target particle as a composite Dirac fermion for concreteness. Some useful insight is gained from the EFT perspective. However, since we exclusively consider the spin-1/2 target particle, the EFT approach itself is unable to account for the specific pattern of target spin dependence at NNLO in heavy target mass expansion observed in this study. Further exploration is needed to understand this issue.

ACKNOWLEDGMENTS

We are grateful for useful discussions with Zhewen Mo, Jichen Pan and Weizhi Xiong.

APPENDIX A: RUTHERFORD SCATTERING WITH MASSLESS SPINLESS PROJECTILE

We can repeat our investigation in Section III.A by replacing the projectile with a massless spin-0 electron, which is described by scalar QED. The electromagnetic vertex involving a scalar electron is simply given by

$$\langle e(k') | J^\mu | e(k) \rangle = -(k^\mu + k'^\mu). \quad (\text{A1})$$

Upon heavy target mass expansion, we again observe that the unpolarized cross sections exhibit some universal feature. Concretely, the LO and NLO pieces in $1/M$ expansion are independent of the target particle spin:

$$\frac{d\sigma}{d\cos\theta} = \frac{\pi\alpha^2 Z^2}{2\mathbf{k}^2 \sin^4\left(\frac{\theta}{2}\right)} - \frac{\pi\alpha^2 Z^2}{M|\mathbf{k}| \sin^2\left(\frac{\theta}{2}\right)} + O\left(\frac{1}{M^2}\right). \quad (\text{A2})$$

The universality becomes partially violated at NNLO. For various target particles, the NNLO contributions are

$$\begin{aligned} \left(\frac{d\sigma}{d\cos\theta}\right)_{\text{NNLO}}^s &= -\frac{4\pi\alpha^2}{M^2 \sin^2\frac{\theta}{2}} \left[F'_{1,0} Z - \Theta\left(s - \frac{1}{2}\right) \frac{s+1}{48s} F_{2,0}^2 (\cos\theta + 1) + \Theta\left(s - \frac{1}{2}\right) \frac{5 - (-1)^{2s}}{24} F_{2,0} Z \right. \\ &\quad \left. + \frac{5}{16} Z^2 \cos\theta - \Theta(s-1) \frac{1}{6} F_{1,1} Z - \frac{1}{12} \left([s] + s + \frac{15}{4} \right) Z^2 \right]. \quad \left(s = 0, \frac{1}{2}, 1, \frac{3}{2}, 2 \right) \end{aligned} \quad (\text{A3})$$

Similar to the pattern indicated in (8) for a massless spin-1/2 projectile, we observe that the $F'_{1,0}Z$, $Z^2 \cos\theta$, and $F_{1,1}Z$ terms are independent of the target spin. The $F'_{1,0}Z$ and $Z^2 \cos\theta$ terms actually have the same origin of the LO and NLO cross sections, which correspond to different terms in the Taylor expansion of $F_{1,0}^2(q^2/M^2)$ in the squared LO amplitude and phase space measure. The coefficient of the $F_{2,0}Z$ term seems to reflect the spin-statistic characteristic of the target particle. For fermions, the coefficient is $1/4$, whereas for bosons, it is $1/6$.

Although the coefficients of $F_{2,0}^2(\cos\theta + 1)$ inside the square brackets explicitly depend on the target spin s , they seem to be expressed as $-\frac{1+s}{48s}$, at least for $s = 1/2, 1, 3/2, 2$. It will be interesting to see whether this parameterization persists for an arbitrary s .

Analogous to what is done in Section III.A, for a spin-1/2 composite target particle, the HPET-based calculation yields the following unpolarized cross section:

$$\frac{d\sigma}{d\cos\theta} = \frac{\pi\alpha^2 Z^2}{2\mathbf{k}^2 \sin^4 \frac{\theta}{2}} - \frac{\pi\alpha^2 Z^2}{M|\mathbf{k}| \sin^2 \frac{\theta}{2}} + \frac{\pi\alpha^2}{4M^2 \sin^2 \frac{\theta}{2}} \times \left[-2c_D Z + c_F^2 (\cos\theta + 1) + 5Z^2 (1 - \cos\theta) \right]. \quad (\text{A4})$$

Reassuringly, this EFT result exactly agrees with that obtained from (A3).

APPENDIX B: RUTHERFORD SCATTERING WITH NONRELATIVISTIC SPINLESS PROJECTILE

We can repeat our investigation in Section III.B by replacing the projectile with a light slowly-moving spinless electron. At the lowest order in electron velocity, but to all orders in $1/M$, the resulting unpolarized cross section is identical to (11), which is obtained for a spin-1/2 projectile. This is well anticipated because the spin degree of freedom decouples in the nonrelativistic limit.

At relative order- v^2 , after heavy target mass expansion, the differential unpolarized cross section becomes particularly simple:

$$\left(\frac{d\sigma}{d\cos\theta} \right)_{(v^2)} = \frac{\pi\alpha^2}{2\mathbf{k}^2 \sin^2 \frac{\theta}{2}} \left[\frac{Z^2}{\sin^2 \frac{\theta}{2}} - \frac{2mZ^2}{M} - \frac{4m^2 Z}{M^2} \tilde{f}_{\text{NNLO}}^s + \mathcal{O}\left(\frac{1}{M^3}\right) \right], \quad (\text{B1})$$

where

$$\tilde{f}_{\text{NNLO}}^s = 2F'_{1,0} + \Theta\left(s - \frac{1}{2}\right) \frac{5 - (-1)^{2s}}{12} F_{2,0} - \Theta(s-1) \frac{1}{3} F_{1,1} + \frac{Z}{4} \cos\theta - \frac{1}{6} \left([s] + s + \frac{2}{3} \right) Z. \quad (\text{B2})$$

$$\left(s = 0, \frac{1}{2}, 1, \frac{3}{2}, 2 \right)$$

Clearly, the $\mathcal{O}(v^2/M^n)$ ($n = 0, 1$) terms remain universal. At $\mathcal{O}(v^2/M^2)$, the universality becomes partially violated. However, the $F'_{1,0}$, $F_{1,1}$, and $Z \cos\theta$ terms still do not depend on the target particle spin. The coefficient of $F_{2,0}$ seems to reflect the spin-statistic characteristic of the tar-

get particle. For fermions, the coefficient is 1/2, whereas for bosons, it is 1/3.

Similar to Section IVB, we can combine NRQED and HPET to study the soft behavior of this type of Rutherford scattering. Since the incident electron is assumed to be spinless, it is natural to work with scalar NRQED plus HPET. Up to the relative order- v^2 , the scalar NRQED Lagrangian reads as

$$\mathcal{L}_{\text{NRQED}} = Q^\dagger \left(iD^0 + d_2 \frac{\mathbf{D}^2}{2m} + d_4 \frac{\mathbf{D}^4}{8m^3} \right) Q, \quad (\text{B3})$$

with Q signifying the field that annihilates a nonrelativistic scalar electron. Again, $d_2 = d_4 = 1$ is a rigorous consequence of Lorentz symmetry.

Based on scalar NRQED and HPET, we are able to obtain the following unpolarized Rutherford cross section, which is accurate to the relative order- v^2/M^2 :

$$\frac{d\sigma}{d\cos\theta} = \frac{\pi\alpha^2 m^2 Z^2}{2\mathbf{k}^4 \sin^4 \frac{\theta}{2}} - \frac{\pi\alpha^2 m^4 Z^2}{M^2 \mathbf{k}^4} + \frac{Z\pi\alpha^2}{2\mathbf{k}^2 \sin^2 \frac{\theta}{2}} \times \left[\frac{Z}{\sin^2 \frac{\theta}{2}} - \frac{2mZ}{M} - \frac{m^2 (-2c_2 Z + c_D + Z \cos\theta + Z)}{M^2} \right]. \quad (\text{B4})$$

Reassuringly, this EFT result exactly reproduces the soft limit obtained from full QED, (B2).

We can further verify that the EFT amplitude reproduces the correct soft behavior, which is deduced by conducting both nonrelativistic and heavy target mass expansion from the full QED amplitude in (1). Working again in Coulomb gauge, and using the following electromagnetic matrix element involving a spinless electron:

$$\langle k' | J^0 | k \rangle = -1, \quad (\text{B5a})$$

$$\langle k' | \mathbf{J} | k \rangle = (\mathbf{k} + \mathbf{k}') \left[\frac{d_2}{2m} - \frac{d_4}{8m^3} (\mathbf{k}^2 + |\mathbf{k}'|^2) \right], \quad (\text{B5b})$$

we can readily obtain the expanded Rutherford amplitude through order- v^2/M^2 , which is indeed compatible with the EFT amplitude.

References

- [1] H. Gegier and E. Marsden, *Proc. R. Soc. Lond. A* **82**, 495 (1909)
- [2] E. Rutherford, *Phil. Mag. Ser. 21*, 669 (1911)
- [3] R. W. Mcallister and R. Hofstadter, *Phys. Rev.* **102**, 851 (1956)
- [4] R. Hofstadter, *Rev. Mod. Phys.* **28**, 214 (1956)
- [5] J. Arrington, W. Melnitchouk, and J. A. Tjon, *Phys. Rev. C* **76**, 035205 (2007)
- [6] F. Gross *et al.*, *Eur. Phys. J. C* **83**, 1125 (2023)
- [7] J. C. Bernauer *et al.*, *Phys. Rev. Lett.* **105**, 1125 (2010)
- [8] W. Xiong *et al.*, *Nature* **575**, 147 (2019)
- [9] M. Mihovilovič, P. Achenbach, T. Beranek, *et al.*, *Eur.*

- [Phys. J. A **57**, 107 \(2015\)](#)
- [10] H. Y. Gao and M. Vanderhaeghen, [Rev. Mod. Phys. **94**, 015002 \(2012\)](#)
- [11] J. P. Karr, D. Marchand, and E. Voutier, [Nat. Rev. Phys. **2**, 601 \(2020\)](#)
- [12] C. Peset, A. Pineda, and O. Tomalak, [Prog. Part. Nucl. Phys. **121**, 103901 \(2021\)](#)
- [13] R. Pohl, A. Antognini, F. Nez, *et al.*, [Nature **466**, 213 \(2010\)](#)
- [14] A. Antognini *et al.*, [Science **101**, 417 \(2013\)](#)
- [15] H. W. Griesshammer, J. A. McGovern, D. R. Phillips, *et al.*, [Prog. Part. Nucl. Phys. **67**, 841 \(2012\)](#)
- [16] F. E. Low, [Phys. Rev. **96**, 1428 \(1954\)](#)
- [17] M. Gell-Mann and M. L. Goldberger, [Phys. Rev. **96**, 1433 \(1954\)](#)
- [18] S. Cotogno, C. Lorc'e, P. Lowdon and M. Morales, [Phys. Rev. D **101**, 056016 \(2020\)](#)
- [19] M. D. Scadron, [Phys. Rev. **165**, 1640 \(1968\)](#)
- [20] D. N. Williams and Y. P. Yao, [Phys. Rev. D **1**, 1380 \(1970\)](#)
- [21] C. Lorce, [arXiv: 0901.4199v1 \[hep-ph\]](#)
- [22] S. Nozawa and D. B. Leinweber, [Phys. Rev. D **42**, 3567 \(1990\)](#)
- [23] F. J. Ernst, R. G. Sachs, and K. C. Wali, [Phys. Rev. **119**, 3567 \(1960\)](#)
- [24] R. G. Sachs, [Phys. Rev. **126**, 2256 \(1962\)](#)
- [25] E. Eichten and B. R. Hill, [Phys. Lett. B **234**, 511 \(1990\)](#)
- [26] H. Georgi, [Phys. Lett. B **240**, 447 \(1990\)](#)
- [27] A. V. Manohar, [Phys. Rev. D **56**, 230 \(1997\)](#)
- [28] W. E. Caswell and G. P. Lepage, [Phys. Lett. B **167**, 437 \(1986\)](#)